Original Article

Sensitivity Laplacian Ratio-Based Optimization of the Projection Selection for Diffuse Optical Tomography

Abstract

Background: In diffuse optical tomography, determining the optimal angle between the source and detector is an effective method to reduce the number of projections while maintaining the quality of the reconstructed images. In this study, a new parameter is introduced to evaluate the source-detector geometries. **Methods:** A two-dimensional mesh with the radius of 20 mm and 7987 nodes were built. In each reconstruction, 0.5 mm heterogeneity with the absorption coefficient of 0.06 mm^{-1} and the dispersion coefficient of 0.6 mm^{-1} was added in different parts of the sample randomly. The relationship between the mean square error (MSE), sensitivity Laplacian ratio (SLR), and sensitivity standard deviation ratio (SSR) was evaluated based on their correlation coefficients. The quality of the images achieved using the optimized projections were compared with that of the full projections for the same depths. **Results:** MSE decreases by increasing the SLR magnitudes which indicate that the parameter could be used to evaluate the scanning geometries. There was a negative correlation coefficient ($R = -0.76$) with the inverse relationship between the SLR and MSE indices. SSR does not have a significant relationship with the quality of the reconstructed images. For each scanning depth, the comparison of the images obtained using the full and optimized-selective projections did not show any considerable difference despite the decrease of the projection numbers in scanning geometry with the optimized-selective projections. **Conclusion:** The unnecessary projections could be eliminated by placing the detectors at the specific angles, which were determined using the SLR. Thus, a proper compromise between the quality of the reconstructed images and reconstruction time might establish.

Keywords: *Diffuse optical tomography, geometry optimization, sensitivity Laplacian ratio, sensitivity standard deviation ratio, source-detector angle*

Anita Ebrahimpour[1],
Seyed Salman
Zakariaee[2],
Marjaneh Hejazi[1]

[1]Department of Medical Physics and Biomedical Engineering, Faculty of Medicine, Tehran University of Medical Sciences, Tehran, [2]Department of Medical Physics, Faculty of Paramedical Sciences, Ilam University of Medical Sciences, Ilam, Iran

Introduction

Optical diffuse tomography is a powerful noninvasive method for animals imaging. Determination of the optimal source-detector geometry has been a challenging topic for many years, because of its close relationship with the quality of the reconstructed images. In pioneer studies, various methods such as singular value analysis (SVD) and orthogonality have been used to evaluate different source-detector geometries and to optimize the parameters such as sampling frequency and field of view. These parameters were applied to the Jacobian matrix.[1-6] These methods were so time-consuming due to the large dimensions of the Jacobian matrix. For solving the time-consuming problem, the number of nodes must be reduced as much as possible, or the simple two- or three-dimensional geometries were used.[7] Furthermore, the mentioned methods (SVD and orthogonality) alone could not evaluate different geometries. They do not change continuously by changing the location of the source-detector due to their mathematical characteristics.[8] In many studies, the uniformity of the sensitivity matrix was used to evaluate different geometries.[9-12] The sensitivity matrix is derived from the sum of the Jacobian matrix rows and represents the sensitivity of the sample points for all of the source-detector pairs. The sensitivity matrix is the function of the imaging geometry and sampling strategy. Therefore, their profiles were drawn for the evaluation of the sensitivity changes.[13-15] The investigation method based on the sensitivity profile is merely a qualitative

How to cite this article: Ebrahimpour A, Zakariaee SS, Hejazi M. Sensitivity laplacian ratio-based optimization of the projection selection for diffuse optical tomography. J Med Signals Sens 2020;10:119-24.

approach and changes must be evaluated quantitatively. The nonuniformity of the sensitivity matrix could be quantitatively calculated using a Laplacian operator, which is considered as an appropriate method for evaluating the source-detector geometries.[8,16] This numerical parameter indicates that an optimal geometry has a uniform sensitivity. However, the nonuniformity of the sensitivity matrix alone cannot provide a precise prediction for the optimal geometry. In the present study, a new parameter is introduced to evaluate the source-detector geometries by considering both the uniformity and mean magnitude of the sensitivity. Based on the proposed method, the optimum angle between the source and detector determined to reduce the number of projections while maintaining the quality of the reconstructed images.

Methods

Description of a new parameter for the geometric evaluation of the optical scanners

For Laplace parameter of p, the photon density in r obtained by the first Born approximation as the following equation:[17]

$$\langle \phi(r,p) \rangle = \langle \phi_{bg}(r,p) \rangle + \phi_{pert}(r,p) \tag{1}$$

Where $\langle \phi_{bg}(r,p) \rangle$ is the background photon density of a homogeneous tissue in r and $\phi_{pert}(r,p)$ is the scattering field due to the perturbation in the optical properties of the tissue. If only the absorption coefficient was taken into account:

$$\phi_{pert}(r,p) = \int_V G_0(r,r_d,p)\delta\mu_a(r)G_0(r,r_s,p)d^3r \tag{2}$$

If the equation was written in the form of a matrix:

$$\phi_{pert} = J\delta \tag{3}$$

Where ϕ_{pert} is a vector with dimensions of M × 1 which represents the detector measurement. δ is the perturbation of the absorption coefficient, and J is the Jacobin matrix which its element described by Eq. 4:

$$J_{i,j} = G_0(r_{di},r_j,p)G_0(r_{si},r_j,p)dv \tag{4}$$

Where r_{si} is the source position in the ith measurement, r_{di} is the detector position in the ith measurement, r_j is the position of the jth voxel, and dv is the voxel size.

For each point, the overall sensitivity matrix achieved by the sum of Jacobian rows (as the Eq. 5). This matrix represents the sensitivity of the point for each pair of the source-detector.[8]

$$S = \sum_{i=1}^{NM} J_{ij} \tag{5}$$

Where S is the sensitivity matrix, and m is the number of source-detector pairs.

Two parameters were introduced to evaluate the sensitivity matrix in different geometric conditions, which were applied to the sensitivity matrix. The sensitivity matrix was first normalized as the Eq. 6:

$$s_{j(n)} = \frac{s_j - min(abs(s_j))}{max(abs(s_j)) - min(abs(s_j))} \tag{6}$$

Where $S_{j(n)}$ is the normalized sensitivity matrix.

The first introduced parameter is sensitivity Laplacian ratio (SLR). This parameter is the ratio of the mean sensitivity to the mean Laplacian applied to the sensitivity.

$$\overline{s_{j(n)}} = \frac{\sum_{j=1}^{n} S_{j(n)}}{n} \tag{7}$$

Where $\overline{s_{j(n)}}$ is the normalized mean sensitivity, and n is the number of voxels.

$$\bar{l} = \frac{|\nabla^2 s_{j(n)}|}{n-2} \tag{8}$$

A Laplacian operator was applied to the sensitivity matrix, which differentiated twice from the discrete space to determine the changes. Then the average of the changes in all adjacent nodes determined to eliminate the error. The SLR parameter was calculated by the following equation:

$$SLR = \frac{\overline{s_{j(n)}}}{\bar{l}} \tag{9}$$

Sensitivity standard deviation ratio (SSR) is the second parameter which proposed for geometry evaluation of the scanning systems. This parameter is the ratio of the mean sensitivity to the standard deviation of the sensitivity matrix:

$$SSR = \frac{\overline{s_{j(n)}}}{\sigma} \tag{10}$$

$$\sigma = \frac{\left(\sum_{j=1}^{n}\left(S_j(n) - \overline{S_j(n)}\right)^2\right)^{1/2}}{n-1} \tag{11}$$

In the Eq. 11, σ is the standard deviation of the sensitivity matrix.

The proposed parameters were evaluated based on their relationship with the quality of the reconstructed images. These assessments were performed using the NIRFAST simulation software (NIRFAST; Dartmouth College and University of Birmingham, Birmingham, UK).[18-20] This software is an open-source light modeling package developed in Dartmouth. In this software, the optical phenomena were simulated based on the finite element method. A two-dimensional mesh with the radius of 20 mm and 7987 nodes (with the absorption coefficient of 0.011 mm^{-1} and the reduced scattering coefficient of 0.33 mm^{-1}) were built. In each reconstruction, 0.5 mm heterogeneity with the absorption coefficient of 0.06 mm^{-1} and the scattering coefficient of 0.6 mm^{-1} was added in different parts of the sample randomly. The source and detector in different geometric conditions, including the different
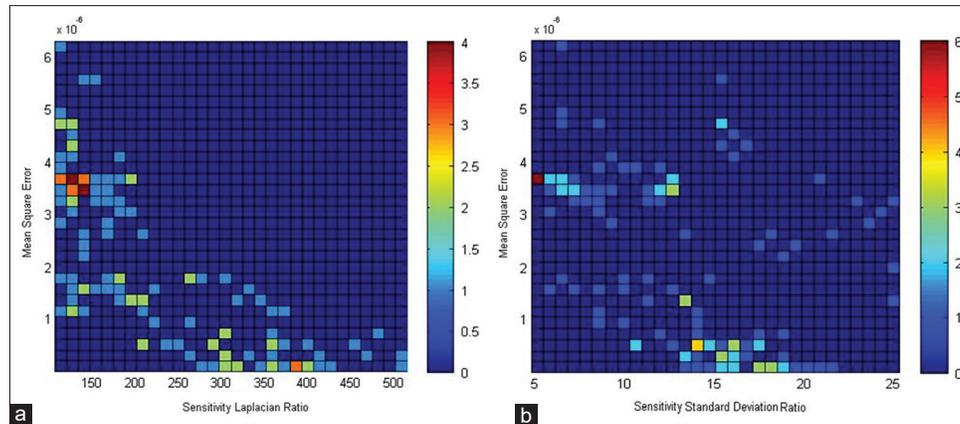
Figure 1: (a) Bin scatter plot between the mean square error of the reconstructed images and sensitivity Laplacian ratio applied to the sensitivity matrix in different source-detector geometries. There was a high correlation coefficient (R = −0.76). (b) Bin scatter plot between the mean square error of the reconstructed images and sensitivity standard deviation ratio applied to the sensitivity matrix in different source-detector geometries. There was a no significant correlation

angles between the source and detector, were simulated randomly. In the present study, 36 sources were located around the sample for all scanning geometries. Then, the forward and reconstruction were performed.[19] For each reconstructed image relate to a special imaging geometry, the mean square error (MSE) was calculated. The MSE is obtained according to the following equation:

$$\text{MSE} = \frac{\sum_{i=1}^{n}(\mu_{ai} - x_{a0,i})^2}{n} \tag{12}$$

Where n is the number of voxels, μ_{ai} is the absorption coefficient of the reconstructed image, and $x_{a0,i}$ is the absorption coefficient of the true image.

For each geometry, the Jacobian matrix was calculated using NIRFAST software. Then, the normalized sensitivity matrix was obtained, and the SLR and SSR parameters were applied. The relationship between the MSE, SLR, and SSR was evaluated based on their correlation coefficients.

Determining the optimal angle between the detector and the source for different depths

After validation of the optimal parameter, it was used to determine the appropriate angle between the source and detector for the different scanning depths. After defining a two-dimensional mesh with the radius of 20 mm, and 7987 nodes (with the absorption coefficient of 0.011 mm^{-1} and the reduced scattering coefficient of 0.33 mm^{-1}), different angles between the source and detector including the 180 degrees (in opposite state) up to 0° (in the consistent situation) with 10° precession were simulated. The mesh depth was divided into 10 separate depths with a 2 mm gap. Jacobian and the sensitivity matrices were calculated for different angles between the source and detector, and the specified region of interests (ROIs) relates to each depth. The verified parameter was separately applied to ROI on the sensitivity map of the scanning depth to find the optimal angles in which the SLR magnitude is maximized.

After determining the optimum angles between the source and detector, the quality of the images achieved using the optimized projections were compared with that of the full projections for the same depth. Four heterogeneities with the radius of 0.5 mm, the absorption coefficient of 0.06 mm^{-1}, and reduced scattering coefficient of 0.6 mm^{-1} were placed in different coordinates of the same depth to cover all points of the depth (for each inhomogeneity, separate reconstruction was performed). For the different samples, the reconstructions were carried out using the mentioned geometries, and the MSE of the reconstructed images was evaluated.

Results

The evaluation of the SSR and MSE indices showed that SSR does not have a significant relationship with the quality of the reconstructed images. There was a negative correlation coefficient (R = −0.76) with the inverse relationship between the SLR and MSE indices [Figure 1].

MSE decreases by increasing the SLR magnitudes which indicate that the parameter could be used to evaluate the scanning geometries. The calculation of SLR index at different angles between the source and detector shows that the maximum SLR for each depth achieved at a particular angle between the source and detector [Figure 2].

For each scanning depth, the comparison of the images obtained using the full and optimized-selective projections did not show any considerable difference [Figure 3]. Reconstructed images for both geometries are shown in Figure 4.

Discussion

In pioneer studies, the nonuniformity of the sensitivity matrix was determined for geometric evaluation of the imaging systems. If there were different sensitivities at the adjacent points with the same absorption and dispersion coefficients, they would be reconstructed with different

optical properties. So that the sensitivity coefficients must be uniform for all sample points.[8] The proposed parameters in the present study indicate that only nonuniformity examination is insufficient for sensitivity assessment of different imaging points. For different scanning points, the average sensitivity increasing is also an important element in the study of the imaging geometry. For the confirmed SLR parameter, the Laplacian operator differentiated twice from the discrete space of the sensitivity. Therefore, this parameter determined minor variations precisely. The

Figure 2: The sensitivity Laplacian ratio magnitudes for the different angles between the source and detector at 10 separate depths. The angles between the source and detector were selected from the 180° angle up to 0° with 10° precession

Figure 3: For two scanning geometries using the full and optimized-selective projections, reconstructions have been made by placing inhomogeneities at 10 separate depths and mean square error of the reconstructed images determined. The horizontal axis denotes the depth number. The sample space is divided into 10 depths with 2 mm gap. Depth numbers increased from the center to the surface

Laplacian operator does not have a specific direction and calculates the changes in all directions. In Eq. 8, after applying the Laplacian operator, an average magnitude determined instead of norm calculation. In the case where the SLR parameter is applied, the possibility of the local error would be eliminated. There was no significant relationship between the SSR parameter and the quality of the reconstructed images due to the mathematical properties of the standard deviation. This parameter calculates the sensitivity variation of the points relative to the mean sensitivity, but the difference in sensitivity for a point relative to its adjacent points is important which could be calculated using the Laplacian operator. For each depth, the optimal angle between the source and detector was determined using the new parameter. The results of the comparison of the reconstructed images for the full and optimized-selective projections show that the number of projections reduced using the optimal geometry while preserving the quality of the reconstructed images. Therefore, computer workload and calculation time reduced. In the present study, the SLR parameter is used to optimize the angle between the source and detector, but this parameter could be used to optimize other geometric parameters such as the number of source-detectors.
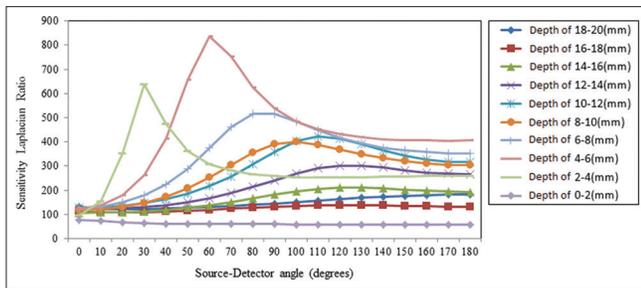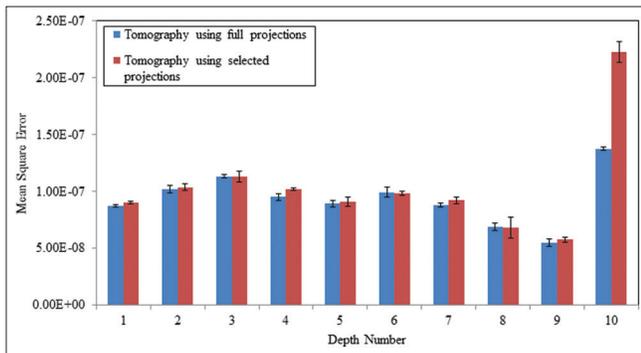
Conclusion

In the diffuse optical tomography, the large numbers of projections increase the duration of the forward stages and reconstruction procedures. Therefore, reducing the number of projections by maintaining the quality of the reconstructed images has a particular importance. The SLR is an applied method to determine the optimal geometry for diffuse optical tomography. The unnecessary projections could be eliminated by placing the detectors at the specific angles; thus, a proper compromise between the quality of the reconstructed images and reconstruction time might establish.
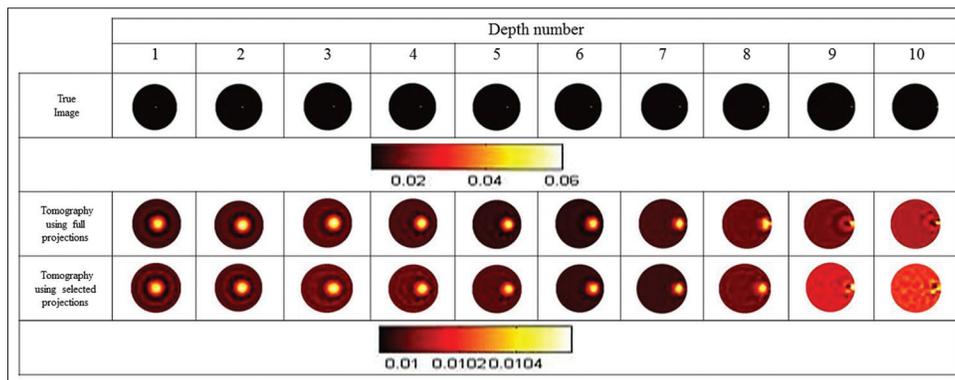
Acknowledgment

Figure 4: The first row of the images represents the true images. The second and third rows represent the reconstructed images. Reconstructions have been made by placing inhomogeneities at 10 separate depths

Conflicts of interest

There are no conflicts of interest.

References

1. Xing X, Lee K, Choe R, Yodh A, editors. Optimization of the Source-detector Geometry for Diffuse Optical Tomography. Biomedical Topical Meeting. Fort Lauderdale, Florida United States: Optical Society of America. 2006. p. 19-22.

2. Serdaroglu A, Yazici B, Kwon K, editors. Optimum Source Design for Detection of Heterogeneities in Diffuse Optical Imaging. Proc SPIE; 2006.

3. Zhang X, Badea C. Effects of sampling strategy on image quality in noncontact panoramic fluorescence diffuse optical tomography for small animal imaging. Opt Express 2009;17:5125-38.

4. Culver JP, Ntziachristos V, Holboke MJ, Yodh AG. Optimization of optode arrangements for diffuse optical tomography: A singular-value analysis. Opt Lett 2001;26:701-3.

5. Xu H, Dehghani H, Pogue BW, Springett R, Paulsen KD, Dunn JF. Near-infrared imaging in the small animal brain: Optimization of fiber positions. J Biomed Opt 2003;8:102-10.

6. Bonfert-Taylor P, Leblond F, Holt RW, Tichauer K, Pogue BW, Taylor EC. Information loss and reconstruction in diffuse fluorescence tomography. J Opt Soc Am A Opt Image Sci Vis 2012;29:321-30.

7. Leblond F, Tichauer KM, Pogue BW. Singular value decomposition metrics show limitations of detector design in diffuse fluorescence tomography. Biomed Opt Express 2010;1:1514-31.

8. Holt RW, Leblond F, Pogue BW, editors. Toward Ideal Imaging Geometry for Recovery Independence Fluorescence Molecular Tomography. Proc SPIE; 2013.

9. Lin ZJ, Niu H, Li L, Liu H. Volumetric diffuse optical tomography for small animals using a CCD-camera-based imaging system. Int J Opt 2012;2012:1-10.

10. Kepshire DS, Davis SC, Dehghani H, Paulsen KD, Pogue BW. Subsurface diffuse optical tomography can localize absorber and fluorescent objects but recovered image sensitivity is nonlinear with depth. Appl Opt 2007;46:1669-78.

11. Tokala KT. A Geometric-Sensitivity-Difference Algorithm for Fluorescence Diffuse Optical Tomography Reconstruction. Oklahoma State University; 2013.

12. Correia T, Banga A, Everdell NL, Gibson AP, Hebden JC. A quantitative assessment of the depth sensitivity of an optical topography system using a solid dynamic tissue-phantom. Phys Med Biol 2009;54:6277-86.

13. Dehghani H, White BR, Zeff BW, Tizzard A, Culver JP. Depth sensitivity and image reconstruction analysis of dense imaging arrays for mapping brain function with diffuse optical tomography. Appl Opt 2009;48:D137-43.

14. Zhan Y, Eggebrecht AT, Culver JP, Dehghani H. Image quality analysis of high-density diffuse optical tomography incorporating a subject-specific head model. Front Neuroenergetics 2012;4:6.

15. Xu G, Piao D. A geometric-sensitivity-difference based algorithm improves object depth-localization for diffuse optical tomography in a circular-array outward-imaging geometry. Med Phys 2013;40:1-18.

16. Holt RW, Leblond FL, Pogue BW. Methodology to optimize detector geometry in fluorescence tomography of tissue using the minimized curvature of the summed diffuse sensitivity projections. J Opt Soc Am A Opt Image Sci Vis 2013;30:1613-9.

17. Chen L, Chen N. Optimization of source and detector configurations based on Cramer-Rao lower bound analysis. J Biomed Opt 2011;16:1-10.

18. Jermyn M, Ghadyani H, Mastanduno MA, Turner W, Davis SC, Dehghani H, *et al*. Fast segmentation and high-quality three-dimensional volume mesh creation from medical images for diffuse optical tomography. J Biomed Opt 2013;18:1-10.

19. Dehghani H, Eames ME, Yalavarthy PK, Davis SC, Srinivasan S, Carpenter CM, *et al*. Near infrared optical tomography using NIRFAST: Algorithm for numerical model and image reconstruction. Commun Numer Methods Eng 2008;25:711-32.

20. Jermyn M, Pogue B, Ghadyani HR, Davis S, Mastanduno MA, Dehghani H, editors. A user-Enabling Visual Workflow for Near-Infrared Light Transport Modeling in Tissue. Biomedical Optics. Miami, Florida, United States: Optical Society of America; 2012.

BIOGRAPHIES

Anita Ebrahimpouris Ph.D. candidate of Medical Physics in Department of Medical Physics of Tehran University of Medical Sciences, Iran. Ebrahimpour received her BSc in Radiologic technology from Iran University of Medical Sciences. She received her Msc in Medical Physics from Tehran University of medical Sciences in 2016.

Email: anitaebrahimpor@gmail.com

Seyed Salman Zakariaee was born in 1987, Sanandaj, Iran. He finished his B.S. in solidstate physics from Urmia University in 2009. Then he followed his postgraduate study in Medical Physics and he was graduated in 2013 from Tabriz University of Medical Sciences. He entered the Ph.D. program of Tehran University of Medical Sciences in the same year and finished his Ph.D. in 2018. He has been working in Medical Physics department of Ilam University of Medical Sciences as assistant professor from 2018.

Email: salman_zakariaee@yahoo.com

Marjaneh Hejazi received her BSc in Radiation Technology from Iran University of Medical Sciences and MSc in Medical Physics from Tehran University of Medical Sciences (TUMS). She graduated on 2004 and continued her academic activity with PhD in Tehran University of Medical Sciences, Medical physics dep., and she is associate professor now.

Email: mhejazi@sina.tums.ac.ir